Shepherd Model for Knot-Limited Polymer Ejection from a Capsid

Tibor Antal[a], P. L. Krapivsky[b], S. Redner[b]

[a]*Program for Evolutionary Dynamics, Harvard University, Cambridge, MA 02138, USA*
[b]*Center for Polymer Studies and Department of Physics, Boston University, Boston, MA 02215, USA*

arXiv:0905.0732v2 [q-bio.QM] 12 Aug 2009

Abstract

We construct a tractable model to describe the rate at which a knotted polymer is ejected from a spherical capsid via a small pore. Knots are too large to fit through the pore and must reptate to the end of the polymer for ejection to occur. The reptation of knots is described by symmetric exclusion on the line, with the internal capsid pressure represented by an additional biased particle that drives knots to the end of the chain. We compute the exact ejection speed for a finite number of knots L and find that it scales as $1/L$. We establish a mapping to the solvable zero-range process. We also construct a continuum theory for many knots that matches the exact discrete theory for large L.

Key words: Virus ejection, Exclusion process, Stochastic effects

1. Introduction

The two basic steps in bacterial infection are the initial injection of the viral DNA into a bacteriophage capsid (Riemer et al., 1978; Kindt et al., 2001; Purohit et al., 2003) and then the ejection of the DNA into a host cell (Inamdar et al., 2006; Castelnovo and Evilevitch, 2007). The processes underlying these two steps are both phenomenologically rich and incompletely understood. In packaging DNA into a capsid, both the strong repulsion from the bending of the DNA and the stress caused by the capsid being smaller than the persistence length have to be overcome. The pressure associated with this capsid packaging can be in the range of tens of atmospheres (Smith et al., 2001; Gelbart and Knobler, 2009). These forces that repel the polymer during packaging are overcome by a specifically-designed motor protein (Inamdar et al., 2006).

The complementary ejection of the DNA into the host cell through small pores in the capsid is driven by the osmotic pressure exerted by the capsid and the internal stresses that have been built up in the highly-confined DNA polymer chain (Inamdar et al., 2006; Gelbart and Knobler, 2009). Because of its central importance in the life cycle of viruses, DNA ejection from a capsid has been intensively studied (Inamdar et al., 2006). Most theoretical treatments have investigated the role of microscopic mechanisms that arise naturally from the combined effects of osmotic pressure and bending energy.

Recent experiments and simulations suggest that viral DNA may become knotted (*i.e.*, a closed chain with a knot cannot be smoothly deformed into a circle) as it is being tightly packed in the capsid (Arsuaga et al., 2002, 2005). These knots are apparently large enough to prevent the DNA from being completely ejected being from the capsid (Mangenot et al., 2005). If this steric hindrance is fully operative, then knots would have to unravel for complete ejection. Because the driving forces are pushing the chain out of the capsid, the only way for complete ejection to occur is for the knot to reptate along the chain and ultimately unravel when the end of the chain is reached. This mechanism and its role on polymer ejection has recently been explored by numerical simulation of a bead-spring model of a flexible polymer together with a coupling to a background solvent (Matthews et al., 2009). This study provides detailed, but nevertheless still qualitative results, for the time dependence of the fraction of the chain that remains within the capsid, as well as the dependence of the ejection time on the number and type of knots on the polymer.

Email addresses: tibor_antal@harvard.edu (Tibor Antal), paulk@bu.edu (P. L. Krapivsky), redner@bu.edu (S. Redner)

In this work, we propose a coarse-grained model to capture the role of knots on the ejection process (Fig. 1). In this model, the reptation of knots is described by the symmetric exclusion process (Harris et al., 1965; Liggett, 1985; Schütz, 2000), while the point at the interface between in the interior and exterior of the capsid undergoes a biased motion and also satisfies the exclusion constraint. We may view this biased particle as a "shepherd" that pushes the knots ("sheep") to the end of the chain where they can unravel. Once all the knots have unraveled, the polymer can be completely ejected.

In the next section, we present the details of this shepherding model. In Sec. 3, we treat the ejection of a polymer chain with a small number of knots. For this discrete system, we write and solve the master equations that describe the position of the knots along the chain. This solution gives the exact result that the velocity of a strongly-biased shepherd equals $1/L$, where L is the number of knots. An unexpected and simplifying feature of the strongly-biased limit is that the velocity and diffusion coefficient of the shepherd do not depend on microscopic rates. We also establish a mapping to the solvable zero range process (Evans and Hanney, 2005), and we use this mapping to obtain further exact results for the diffusion of the shepherd. Finally, we investigate a semi-infinite system with a finite density of knots (Sec. 4). Here we apply a continuum approach to solve for the knot density profile, from which the displacement of the shepherd grows as $\sqrt{A\,t}$, with a calculable amplitude A.

2. Model

To present our model, it is convenient to employ a reference frame that is fixed along the length of the polymer. The chain can be divided into a portion that has been ejected from the capsid and the portion that remains in the interior. The basic feature of our modeling is that ejection may be hindered by the existence of knots along the portion of the polymer that is still inside the capsid. We assume that these knots are sufficiently large that they cannot pass through the pore in the capsid (Matthews et al., 2009). Because of this restriction, some other relaxation mechanism is needed to allow for complete ejection of a polymer.

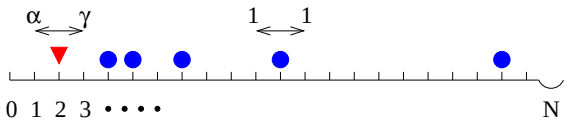

Figure 1: Schematic illustration of the shepherding process. The motion of the shepherd (▼) is biased to the right, while the knots (•) are represented as localized particles that hop symmetrically on the integer interval $[0, N]$. Upon reaching the end of the chain, the knot has unraveled; this event is represented as an absorbing boundary at N.

One such mechanism is provided by the possibility that knots are not static but move along the polymer chain by reptation (Matthews et al., 2009). When a knot reptates to the free end of the polymer, it disappears because the entanglement of the knot is released. If the chain contains multiple knots, then we assume that they cannot pass through each other; instead they must individually reptate to the end of the chain and unravel in sequence.

Our main focus is the position of the point that separates the ejected portion of the polymer from the portion inside. We model the position of this dividing point by an effective particle (a "shepherd") that undergoes biased diffusion along the chain, with rates α and $\gamma > \alpha$ to the left and right, respectively. The bias of the shepherd corresponds to the polymer being pushed out of the capsid by osmotic pressure and the release of bending energy. The shepherd therefore rectifies the diffusive motion of the knots so that the polymer will be ejected. When the shepherd reaches the right end of the polymer, the ejection is complete. In the spirit of minimalism, we assume that this bias is constant throughout the ejection process; in reality the bias will decrease with time as the ejection of the polymer relaxes the stresses that drives the ejection.

We assume that the chain initially contains a specified number of knots that are randomly interspersed along the chain. The ejected portion is necessarily free of knots, while the complementary portion of the chain remains knotted (except possibly near the very end of the ejection process). In the spirit of a coarse-grained model, we ignore the topology of the knots and replace them by localized defects. Each defect can move equally likely in both direction along the chain due to thermal noise, and hence the reptation of the knot is modeled as a symmetric random walk. Different type of knots could be described by different diffusion coefficients, however, we restrict our discussion to a single type of knot, where all knots have the same hopping rates. In addition to the random motion of the knots, there

is also an exclusion constraint because knots cannot pass through each other or pass by the shepherd (corresponding to the disallowed event of a knot passing through the capsid pore). The knots can be viewed as a flock of diffusing and mutually repelling excitations that are pushed to the end of the interval by an advancing shepherd. When each knot reaches the right end of the chain it simply disappears, corresponding to an absorbing boundary condition. When the shepherd reaches the end of the chain (Fig. 1), the polymer has been completely ejected.

Because of its bias, the shepherd rectifies the diffusive motion of the knots. This rectification of thermal noise underlies many microscopic biological processes, such as the motion of motor proteins (Howard, 2001), and the chaperon assisted translocation of polymers across a membrane (D'Orsogna et al., 2007). In our model of polymer ejection, the rectification is mediated by the exclusion constraint of the knots, leading to an exclusion process in which a single particle is subject to a bias that acts indirectly on all other particles. A two-sided version of this model with a biased particle caged in between unbiased particles has been studied previously (Burlatsky et al., 1992a, 1996; Landim et al., 1998); this model mimics, *e.g.*, the field-driven motion of a charged particle that is immersed in a lattice gas of neutral particles. It is worth mentioning that various embellishments of idealized exclusion processes have helped to understand a variety of biological processes and have raised new theoretical questions about the exclusion process itself (Reichenbach et al., 2006; Stukalin et al., 2006; Dong et al., 2007; Antal et al., 2007).

3. Discrete Formulation

We first study the case of a small number of knots by writing the discrete master equations that describe the probability distribution for their positions. These master equations turn out to be soluble, from which we can extract the speed of the shepherd in the steady state.

3.1. Single Knot

To determine the ejection speed of a polymer that contains a single knot, note that before the shepherd first reaches the knot, its speed is simply $v_0 = \gamma - \alpha$ (Fig. 2, left). Subsequently, the knot and the shepherd stay close to each other because of the bias of the shepherd toward the knot. As a result, the speed of their mutual advance is less than v_0. To obtain this speed, we define $P(n)$ as the probability that the number of empty sites between the shepherd and the first knot is n. We call this number of vacancies between the two particles as the "gap". For gap size $n \geq 0$, n can increase to $n + 1$ with rate $1 + \alpha$, either by the knot hopping one step to the right or the shepherd hopping one step to the left with rate α, respectively. Similarly, for $n \geq 1$, the gap size n decreases to $n - 1$ with rate $1 + \gamma$. When $n = 0$, the gap size can only increase with rate $1 + \alpha$.

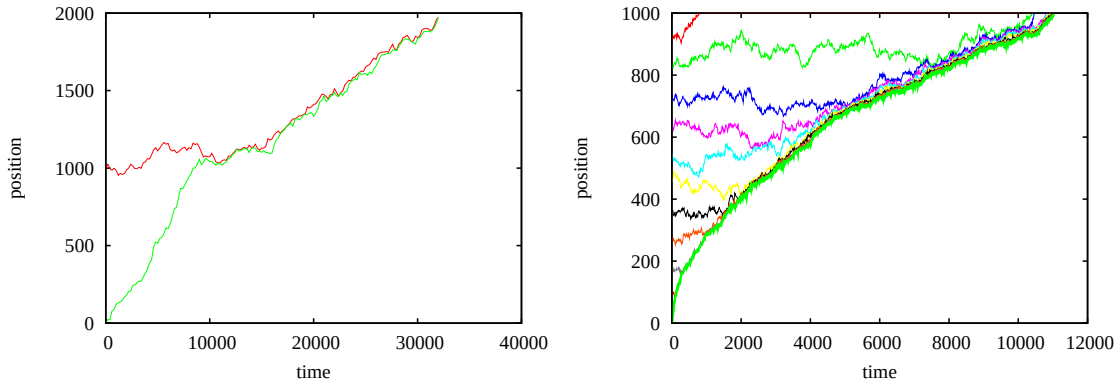

Figure 2: (Left) Time dependence of the positions of the shepherd (lower) and a single knot (upper), when the shepherd hopping rates to the right and left are $\gamma = 1.1$ and $\alpha = 1$, respectively. (Right) Time dependence of the positions of the shepherd (lower) and 10 knots (upper) on a chain of length 1000, when the shepherd hopping rates to the right and left are $\gamma = 2$ and $\alpha = 1$, respectively.

Because the shepherd is driven toward the knot for $\gamma > \alpha$, the distance distribution between these two entities reaches a steady state. In this state, the two transition rates $(1 + \alpha)P(n)$ and $(1 + \gamma)P(n + 1)$ are equal and give the

recursion, for $n \geq 0$, $(1+\alpha)P(n) = (1+\gamma)P(n+1)$ for $n \geq 0$, with solution

$$P(n) = \frac{\gamma - \alpha}{\gamma + 1}\left(\frac{1+\alpha}{1+\gamma}\right)^n . \tag{1}$$

Here the overall amplitude is determined by the normalization condition $\sum_{n\geq 0} P(n) = 1$.

Since the shepherd can always hop to the left (with rate α), but it can hop to the right only if its right neighbor is empty (probability $1 - P_0$) , the speed of the shepherd for the case of one knot is

$$V_1 = \gamma(1 - P_0) - \alpha = \gamma\frac{1+\alpha}{1+\gamma} - \alpha\,, \tag{2}$$

In the limit of an infinitely biased shepherd ($\gamma \to \infty$), Eq. (2) reduces to $V_1 = 1$.

3.2. Several Knots

For L knots their configuration may be specified by the set of separations $\mathbf{n} \equiv (n_1, n_2, \ldots, n_L)$, where n_i is the number of vacancies to the left of the i^{th} knot. The stationary probability $P(\mathbf{n})$ for a configuration specified by $\mathbf{n}$ satisfies the equation

$$\begin{aligned}\frac{dP(\mathbf{n})}{dt} &= -(\alpha+\gamma+2L)P(\mathbf{n}) + \gamma P(n_1+1) + \alpha P(n_1-1) \\ &\quad + \sum_{k=1}^{L-1}\Big[P(n_k - 1, n_{k+1}+1) + P(n_k+1, n_{k+1}-1)\Big] + P(n_L - 1) + P(n_L + 1) = 0\,.\end{aligned} \tag{3}$$

The scalar arguments of P on the right-hand side indicate that only the components of the separation vector that have been changed from those in $\mathbf{n}$. Equation (3) is valid for configurations in which the separations between consecutive knots are all at least one ($n_k \geq 1$ for every k). For configurations where some $n_k = 0$ (*i.e.*, zero separation between adjacent knots), the relevant separations cannot decrease. In such cases and independently for each k, the following terms are missing (*i.e.*, they should be subtracted) from the right-hand side of (3)

$$\begin{array}{ll} -(1+\gamma)P(\mathbf{n}) + \alpha P(n_1-1) + P(n_1-1, n_2+1) & \text{for } k = 1 \\ -2P(\mathbf{n}) + P(n_{k-1}+1, n_k - 1) + P(n_k - 1, n_{k+1}+1) & \text{for } 2 \leq k \leq L-1 \\ -2P(\mathbf{n}) + P(n_{L-1}+1, n_L - 1) + P(n_L - 1) & \text{for } k = L. \end{array} \tag{4}$$

(Here we formally allow n_k to take the value -1 for convenience.) By solving the system of equations (3) and (4) for a small number of knots, a simple pattern emerges that suggests that the exact solution factorizes and individual gaps are distributed according to exponential distributions

$$P(\mathbf{n}) = \prod_{k=1}^{L}(1 - z_k)\, z_k^{n_k}\,. \tag{5}$$

(The prefactor in (5) assures that normalization is obeyed: $\sum P(\mathbf{n}) = 1$.) Substituting ansatz (5) into the bulk and boundary equations, Eqs. (3) and (4), we obtain

$$\alpha + \gamma + 4 = \gamma z_1 + \frac{\alpha + z_2}{z_1} + \frac{z_{L-1}+1}{z_L} + z_L + \sum_{k=2}^{L-1}\frac{z_{k-1} - 2z_k + z_{k+1}}{z_k}, \tag{6}$$

as well as

$$\begin{array}{ll} z_1(1+\gamma) = \alpha + z_2\,, & \text{for } k = 1 \\ 2z_k = z_{k-1} + z_{k+1}, & \text{for } 2 \leq k \leq L-1 \\ 2z_L = z_{L-1} + 1\,, & \text{for } k = L \end{array} \tag{7}$$

When the conditions (6) and (7) are both satisfied the solution is stationary. Equation (7) represents a linear recursion with the unique solution

$$z_k = \frac{\alpha L + 1 + (\gamma - \alpha)(k-1)}{\gamma L + 1}\,. \tag{8}$$

This form for z_k also satisfies the bulk equation (6), which can be verified by substitution.

The speed of the shepherd can be calculated in the same way as in the case of a single knot. The shepherd can always jump to the left, but it can jump to right only if its right neighbor is empty, that is $V_L = \gamma \text{Prob}(n_1 \geq 1) - \alpha$. The probability that the first gap has size of at least one is

$$\text{Prob}(n_1 \geq 1) = (1 - z_1) \sum_{n_1=1}^{\infty} z_1^{n_1} = z_1 \ . \tag{9}$$

Hence the speed of the shepherd is

$$V_L = \frac{\gamma - \alpha}{\gamma L + 1} \ . \tag{10}$$

Equation (5) shows that the probability distribution for the gap size $\ell_k = 1 + n_k$ between the $(k-1)^{\text{st}}$ and k^{th} knots is $(1 - z_k)\, z_k^{\ell_k - 1}$ and therefore the average distance is

$$\langle \ell_k \rangle = \sum_{\ell_k \geq 1} \ell_k \, (1 - z_k)\, z_k^{\ell_k - 1} = \frac{1}{1 - z_k} = \frac{\gamma L + 1}{\gamma - \alpha} \, \frac{1}{L - k + 1} \tag{11}$$

Since gaps are independent, the average total size (*i.e.*, the average distance between the shepherd and the L^{th} knot) is

$$\langle \ell \rangle = \sum_{k=1}^{L} \langle \ell_k \rangle = \frac{\gamma L + 1}{\gamma - \alpha} \, H_L \tag{12}$$

where $H_L = \sum_{1 \leq j \leq L} j^{-1}$ are harmonic numbers. Using the asymptotic $H_L \simeq \ln L$ when $L \gg 1$ we see that the average gap size scales according to

$$\langle \ell \rangle \simeq \frac{\gamma}{\gamma - \alpha} \, L \ln L \tag{13}$$

when the number of knots is large. Similarly, we use the independence of gaps to compute the variance of the total size

$$\langle \ell^2 \rangle - \langle \ell \rangle^2 = \sum_{k=1}^{L} \left[\langle \ell_k^2 \rangle - \langle \ell_k \rangle^2 \right] = \sum_{k=1}^{L} \frac{z_k}{(1 - z_k)^2} \tag{14}$$

which simplifies [upon using (8)] to

$$\langle \ell^2 \rangle - \langle \ell \rangle^2 = \left(\frac{\gamma L + 1}{\gamma - \alpha} \right)^2 H_L^{(2)} - \frac{\gamma L + 1}{\gamma - \alpha} \, H_L \tag{15}$$

where $H_L^{(2)} = \sum_{1 \leq j \leq L} j^{-2}$. For large number of knots $H_L^{(2)} \to \pi^2/6$ and therefore asymptotically

$$\langle \ell^2 \rangle - \langle \ell \rangle^2 = \frac{\pi^2}{6} \left(\frac{\gamma}{\gamma - \alpha} \right)^2 L^2 + O(L \ln L) \tag{16}$$

Hence the relative fluctuations of the total size diminish, albeit slowly as the inverse logarithm of the total number of knots:

$$\frac{\sqrt{\langle \ell^2 \rangle - \langle \ell \rangle^2}}{\langle \ell \rangle} \sim \frac{1}{\ln L} \tag{17}$$

In the special case of an infinitely biased shepherd ($\gamma = \infty$), the shepherd is always adjacent to the first knot, so that $n_1 = 0$ and the stationary probability (5), (8) becomes

$$P(\mathbf{n}) = \prod_{k=2}^{L} \left(\frac{k-1}{L} \right)^{\ell_k} \ . \tag{18}$$

In this limit, the speed of the shepherd reduces to $V_L = 1/L$ and other characteristics of the system similarly simplify.

A useful feature of our model is that it can be mapped onto the *zero range process* (ZRP) (Evans and Hanney, 2005) on a chain of L sites with open boundaries. In this mapping, each knot corresponds to a site in the ZRP, and the number n_k of empty sites to the left of each knot corresponds to the number of particles that occupy site k in the ZRP. The particles in the ZRP multiply occupy each site, and only the top particle can hop at a rate that is independent of the occupancy of the target site. For example, knot k hopping to the right corresponds to a particle in the ZRP hopping from site $k+1$ to k. The top particle in this corresponding ZRP can hop: (i) both to the left and to the right at rate 1 from each bulk site; (ii) out of site $k = 1$ at rate γ and into $k = 1$ at rate α; (iii) either in or out of site $k = L$ at rate 1. The relevant feature of this mapping is that the negative of the current entering the ZRP from the left exactly corresponds to the speed of the shepherd.

Our shepherd model is a special case of the general ZRP that was solved by Levine et al. (2005) and Eqs. (5), (8), and (10) are special cases of their solution. In addition to its average speed, we are also interested in the diffusion coefficient of the shepherd. Due to the equivalence of the models, the negative time integrated current $-J(t)$ of the ZRP corresponds to the position $x(t) = -J(t)$ of the shepherd in our model. We can use results of Harris et al. (2005) for the fluctuations of the time-integrated current. From this work, the large time asymptotic of the Laplace transform of the position of the shepherd is given explicitly by (the large-L limit of the expression below was obtained previously in Bodineau and Derrida (2004); Wijland and Rácz (2005)):

$$\hat{x}(\lambda) \equiv \lim_{t\to\infty} \frac{1}{t} \log\langle e^{-\lambda x(t)}\rangle = \frac{(1-e^{\lambda})(\alpha e^{-\lambda}-\gamma)}{1+\gamma L} \,. \tag{19}$$

From this equation, the speed of the shepherd (10) can be obtained as $V_L = \partial_\lambda \hat{x}|_{\lambda=0}$, while the diffusion coefficient is

$$D_L = \frac{1}{2} \left.\frac{\partial^2 \hat{x}}{\partial \lambda^2}\right|_{\lambda=0} = \frac{\alpha+\gamma}{2(1+\gamma L)} \tag{20}$$

Again, the result is particularly neat, $D_L = (2L)^{-1}$, in the limit of an infinitely biased shepherd.

3.3. Ejection Time

What is the average ejection time of a polymer with a finite density of knots? For concreteness, consider a polymer of length N, with a shepherd at site 0, and L equidistant knots initially at $x_i = iN/(L+1)$, $i = 1, \ldots, L$. If the knot density $\rho_\infty = L/N$ is sufficiently low (roughly if $\rho_\infty \ll \gamma - \alpha$), the biased shepherd reaches each knot close to the knot's initial position. The shepherd advances with the localized flock of k already-collected knots with asymptotic speed $V_k = (\gamma-\alpha)/(\gamma k+1)$, see Eq. (10), until the flock reaches the $(k+1)^{\text{st}}$ knot. Consequently, the time for the shepherd to reach the end of the polymer is

$$t = \frac{N}{L+1} \sum_{k=0}^{L} \frac{1}{V_k} = \frac{N}{2} \frac{\gamma L+2}{\gamma-\alpha} \tag{21}$$

Simulation results for this time are plotted in Fig. 3 for a polymer of length $N = 100$ as a function of the number of knots when the bias of the shepherd is weak ($\alpha = 1, \gamma = 2$). Our result (21) gives an excellent fit to the data even for this short polymer.

For a finite density of knots $\rho_\infty = L/N$, we also obtain the asymptotic position of the shepherd from (21) as

$$x \simeq \sqrt{\frac{2(\gamma-\alpha)}{\gamma\rho_\infty}\, t} \;\longrightarrow\; \sqrt{2t/\rho_\infty} \qquad \alpha \to 0 \,. \tag{22}$$

Notice the lack of dependence on the hopping rate γ of the shepherd in the asymmetric limit of $\alpha \to 0$.

When a real virus is ejected from the capsid, the pressure should decrease during this process (Gelbart and Knobler, 2009). This effect can be modeled as a decreasing bias γ for the shepherd. Since the bias is so enormous in the capsid (Gelbart and Knobler, 2009), even the decreased bias can be considered as large bias in our model. This argument is supported by the fairly uniform rate of virus ejection in simulations of Matthews et al. (2009). The ejection time (21) for large bias becomes $t = NL/2$, that is independent of the rates α and γ. Knowing this ejection time experimentally would give us an estimate for the hopping rates of the knots, (which we used to rescale time with). Unfortunately, we do not know of such experiments.

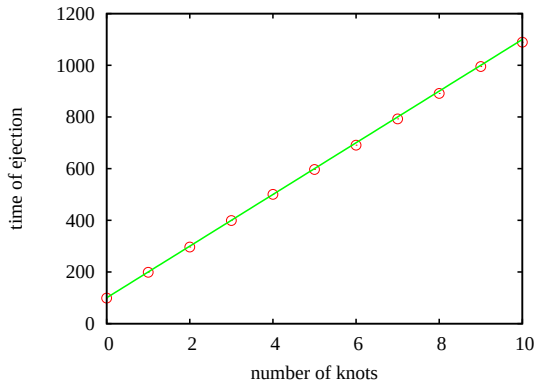

Figure 3: Average ejection time for a polymer of length 100 as a function of the number of equidistant knots L. The hopping rates of the shepherd are $\alpha = 1$, $\gamma = 2$. The line is the function $100 * (1 + L)$ as given by Eq. (21).

4. Finite Density of Knots

When the number of knots is large, it is more convenient to study the knot density profile by a continuum theory. While a finite knot density is perhaps not of direct relevance to the polymer ejection problem, this limiting situation leads to an appealing exclusion process that can be solved in a simple way by applying a scaling approach to account for the effective moving boundary condition caused by the motion of the shepherd (Crank, 1987).

Let $\rho(x,t)$ denote the continuum knot density at position x and time t, and let $x_*(t)$ denote the position of the shepherd (Fig. 4). Initially the shepherd is at $x_* = 0$ and it hops to the right with rate 1 whenever its right neighbor is vacant. In the continuum limit, the knot density $\rho(x,t)$ satisfies the diffusion equation

$$\frac{\partial \rho}{\partial t} = \frac{\partial^2 \rho}{\partial x^2}\ . \tag{23}$$

The diffusion coefficient $D = 1$ since the hopping rate of each knot equals 1 and the exclusion plays no role in the overall density when the hopping is symmetric (Schütz, 2000).

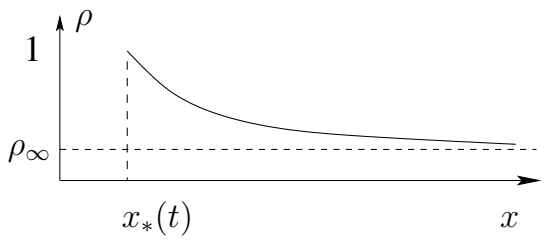

Figure 4: Sketch of the knot density as a function of position along the chain in the continuum limit.

As the shepherd advances, knots accumulate in front of it and the knot density increases monotonically from a value ρ_∞ as $x \to \infty$ to the value 1 at x_*. The shepherd advances only when the adjacent site is empty. In the continuum limit, the analog of this advancement rule is

$$\frac{dx_*}{dt} = -\frac{\partial \rho}{\partial x}\Big|_{x=x_*}. \tag{24}$$

That is, the probability that there is a gap in front of the shepherd equals the local knot density gradient. Thus we must solve the diffusion equation (23) in the region $x_*(t) < x < \infty$ subject to the initial condition $\rho(x > 0, 0) = \rho_\infty$ and the boundary condition $\rho(x_*, t > 0) = 1$.

This type of moving boundary-value, or Stefan, problem (Crank, 1987; Langer, 1987) can be solved by a scaling approach. Let us assume that the density profile approaches the scaling form

$$\rho(x,t) = f(\xi), \quad \text{where} \qquad \xi = \frac{x}{x_*} - 1\,. \tag{25}$$

Using this scaling form, the derivatives of the density are:

$$\frac{\partial\rho}{\partial t} = -\frac{\dot{x}_*}{x_*}(1+\xi)f', \quad \frac{\partial\rho}{\partial x} = \frac{1}{x_*}\,f', \quad \frac{\partial^2\rho}{\partial x^2} = \frac{1}{x_*^2}\,f''\,.$$

Using these, the diffusion equation (23) can be written in the separated form

$$\dot{x}_* x_* = -\frac{f''(\xi)}{(1+\xi)f'(\xi)},$$

where A is a separation constant. Equation (24) for the motion of the boundary gives

$$x_*\,\dot{x}_* = -f'(0)\,, \tag{26}$$

which both fixes the separation constant $A = -f'(0)$ and implies that the boundary point advances in time as

$$x_* = \sqrt{2At}\,. \tag{27}$$

In scaled coordinates the differential equation for the density profile now becomes $f''(\xi) = -A(1+\xi)f'(\xi)$. Integrating this equation, subject to the boundary condition $\rho(x_*, t>0) = 1$ (or $f(0) = 1$), yields

$$f(\xi) = 1 - A\int_0^\xi d\eta\, e^{-A(\eta+\eta^2/2)}\,. \tag{28}$$

To eliminate the unknown constant $A = -f'(0)$, we use the fact that $f(\infty) = \rho_\infty$ to obtain the relation

$$\begin{aligned}\rho_\infty &= 1 - A\int_0^\infty d\eta\; e^{-A(\eta+\eta^2/2)} \\ &= 1 - \sqrt{\pi A/2}\; e^{A/2}\;\mathrm{erfc}(\sqrt{A/2}).\end{aligned}$$

that (implicitly) determines A as a function of ρ_∞; here erfc is the complementary error function (Abramowitz and Stegun, 1972). Using the asymptotic forms of the error function, we can extract the limiting behaviors of the separation constant A, from which the position of shepherd is given by

$$x_* \simeq \sqrt{t} \times \begin{cases} \sqrt{2/\rho_\infty} & \rho_\infty \downarrow 0 \\ 2\pi^{-1/2}(1-\rho_\infty) & \rho_\infty \uparrow 1\,. \end{cases} \tag{29}$$

Notice that the limiting expression for $\rho_\infty \to 0$ reproduces Eq. (22) that we obtained from the exact discrete solution.

5. Summary

We modeled the ejection of a knotted flexible polymer from a capsid in terms of a hybrid dynamical model that consists of a single asymmetric exclusion process (representing the boundary point on the polymer between the interior and exterior of the capsid) that interacts with a gas of symmetric exclusion processes (the knots). In the absence of any external forces, the knots reptate symmetrically along the chain. The effect of the osmotic pressure is modeled as the single asymmetric exclusion process that shepherds the knots to the opposite end of the chain where their entanglement is released. Once all the knots have unraveled, the polymer can be ejected.

The ejection speed V_L can be solved exactly for the $L+1$-particle system that consists of the shepherd and L knots and the result is remarkably simple for a strongly-biased shepherd: $V_L = 1/L$. The underlying exclusion process

can also be solved for a finite density of knots by a continuum description. Here the amount of the chain that is ejected at time t is not proportional to t, but rather to $\sqrt{t}$. This behavior matches that of the discrete solution in the limit of a strongly-biased shepherd. In all of our theoretical modeling, we use constant bias throughout the entire ejection process. We argue that the motion remains in the strong-bias regime throughout the ejection process due to the extremely large initial pressure in the capsid. As long as the system remains in this strong-bias limit, the motion of the shepherd and the knots are not influenced by the decrease in the ejection force and it is appropriate to treat the bias as constant.

One final point is that we have assumed that all knots are identical. It may be worthwhile to extend our model to the physical more realistic case where knots are non-identical, so that their diffusivities are random variables.

Acknowledgments

We thank Gleb Oshanin for useful correspondence about lattice gases. We are grateful for financial support from NIH grant R01GM078986 (TA), NSF grants CCF-0829541 (PLK) and DMR0535503 (SR).

References

Abramowitz M., Stegun I. A., 1972. Handbook of Mathematical Functions. Dover, New York.

Antal T., Krapivsky P. L., Mallick K., 2007. Molecular spiders in one dimension. J. Stat. Mech. P08027.

Arsuaga J., Vazquez M., Trigueros S., Sumners D.W., Roca J., 2002. Knotting probability of DNA molecules confined in restricted volumes: DNA knotting in phage capsids. Proc. Natl. Acad. Sci. U.S.A. **99**, 5373–5377.

Arsuaga J., Vazquez M., McGuirk P., Trigueros S., Sumners D. W., Roca J., 2005. DNA knots reveal a chiral organization of DNA in phage capsids. Proc. Natl. Acad. Sci. U.S.A. **102**, 9165–9169.

Bodineau T., Derrida B., 2004. Current fluctuations in nonequilibrium diffusive systems: An additivity principle. Phys. Rev. Lett. **92**, 180601.

Burlatsky S. F., Oshanin G. S., Mogutov A. V., Moreau M., 1992. Directed walk in a one-dimensional lattice gas. Phys. Lett. A **166**, 230–234.

Burlatsky S. F., Oshanin G. S., Moreau M., Reinhardt W. P., 1996. Motion of a driven tracer particle in a one-dimensional symmetric lattice gas. Phys. Rev. E **54**, 3165–3172.

Castelnovo M., Evilevitch A., 2007. DNA ejection from bacteriophage: Towards a general behavior for osmotic-suppression experiments. Eur. Phys. J. E **24**, 9–18.

Crank J., 1987. Free and Moving Boundary Problems. Oxford University Press, Oxford.

Dong J. J., Schmittmann B., Zia R. K. P., 2007. Towards a model for protein production rates. J. Stat. Phys. **128**, 21–34.

D'Orsogna M. R., Chou T., Antal T., 2007. Exact steady-state velocity of ratchets driven by random sequential adsorption. J. Phys. A **40**, 5575–5584.

Evans M. R., Hanney T., 2005. Nonequilibrium statistical mechanics of the zero-range process and related models. J. Phys. A **38**, R195–R240.

Gelbart, W. M., Knobler C. M., 2009. Pressurized viruses. Science **323**, 1682–1683.

Harris T. E., 1965. Diffusions with collisions between particles. J. Appl. Prob. **2**, 323–338.

Harris R. J., Rakos A., Schütz G. M., 2005. Current fluctuations in the zero-range process with open boundaries. J. Stat. Mech. P08003.

Howard J., 2001. Mechanics of Motor Proteins and the Cytoskeleton. Sinauer Associates, Sunderland, MA.

Inamdar M., Gelbart W. M., Phillips R., 2006. Dynamics of DNA ejection from bacteriophage. Biophys. J. **91**, 411–420.

Kindt J. T., Tzlil S., Ben-Shaul A., Gelbart W. M., 2001. DNA packaging and ejection forces in bacteriophage. Proc. Natl. Acad. Sci. (USA) **98**, 13671–13674.

Landim C., Olla S., Volchan S. B., 1998. Driven tracer particle in one-dimensional symmetric simple exclusion. Commun. Math. Phys. **192**, 287–307.

Langer J. S., 1987. Lectures in the theory of pattern formation. In: Chance and Matter, eds. Souletie J., Vannimenus J., Stora R., North-Holland, Amsterdam.

Levine E., Mukamel D., Schütz G. M., 2005. Zero-range process with open boundaries. J. Stat. Phys. **30**, 759–778.

Liggett T. M., 1985. Interacting Particle Systems. Springer, Berlin.

Mangenot S., Hochrein M., Radler J., Letellier L., 2005. Real-time imaging of DNA ejection from single phage particles. Curr. Biol. **15**, 430.

Matthews R., Louis A. A., Yeomans J. M., 2009. Knot-controlled ejection of a polymer from a virus capsid. Phys. Rev. Lett. **102**, 088101.

Purohit P. K., Kondev J., Phillips R., 2003. Mechanics of DNA packaging in viruses. Proc. Natl. Acad. Sci. U.S.A. **100**, 3173–3178.

Reichenbach T., Franosch T., Frey E., 2006. Exclusion processes with internal states. Phys. Rev. Lett. **97**, 050603.

Riemer S. C., Bloomfield V. A., 1978. Packaging DNA in bacteriophage heads – some considerations on energetics. Biopolymers **17**, 785–794.

Schütz G. M., 2000. In: Phase Transitions and Critical Phenomena. Vol. 19, C. Domb, J. L. Lebowitz, eds., Academic Press, London.

Smith D. E., Tans S. J., Smith S. B., Grimes S., Anderson D. L., Bustamante C., 2001. The bacteriophage f29 portal motor can package DNA against a large internal force. Nature **413**, 748–752.

Stukalin E. B., Kolomeisky A. B., 2006. Transport of single molecules along the periodic parallel lattices with coupling. J. Chem. Phys. **124**, 204901.

van Wijland F., Rácz Z., 2005. Large deviations in weakly interacting boundary driven lattice gases. J. Stat. Phys. **118**, 27–54.